S1. Analysis of the force curves. Calibrations.

The upper panel of Fig.S1 shows a raw force curve as obtained from the software NanoScope: laser deflection on the detector (reported as a potential in V) as a function of the movement of the piezoelectric in the z direction informed as a distance (z_{piezo}). The lower panel shows the same curves in a more usual format: force (in N) as a function of indentation depth (z_{tip}).

In the approach portion of the force curve (blue curves in the figure), we can identify the following regions:

i) Non-contact region (A in Fig. S1).

ii) An acute jump towards negative potentials, known as jump-in or jump-to-contact. This jump is attributed to the presence of attractive forces (electrostatic or capillary in many cases) between the tip and the sample, which at point B (Fig. S1) become large enough to induce the flexion of the cantilever.

iii) The jump stops when the tip gets into contact with the solid substrate (C in Fig. S1). Some authors argue that forces on the tip might equilibrate before contact (due to repulsive forces or the presence of a liquid layer) or after contact (after indenting several layers of the solid). (Pittenger et al, 2001)

iv) Contact region. The cantilever flexes upwards, exerting an increasing force over the substrate (D in Fig. S1). Depending on other existing forces, and the mechanical properties of the sample, this can produce different effects: no deformation (left panel), elastic or plastic deformation (right panel), viscous flow, etc.

The retract portion of the curve (green curves in Fig. S1) is very similar to the approach portion. In the region E, the cantilever force overcomes the pull-off force (also called adhesion force) and causes another jump.

Quantitative analysis of force curves requires several calibrations. The piezoelectric was periodically calibrated in x, y and z directions using Nanoscope 5.30r3 and a commercial calibration grid (Veeco VGRP-15M, platinum covered silicon, with square pits of 10 µm x 10 µm and 180 nm depth). This assures accuracy on the z_{piezo} coordinate (upper panel, Fig. S1).

Raw deflection (informed as a potential between -9.68 and +9.68 V) must be converted to deflection distance. For this, we measured force curves on "infinitely hard" substrates (mica, in this case). Then, we analyzed those curves under the assumption that in the contact region (Fig. S1, region D in left panels, and diagram D.i) there is no indentation of the sample (Butt et al., 2005). Thus, the true distance between the tip and the sample remains constant: the piezoelectric displacement is compensated by the cantilever deflection. Hence, the slope of this region of the force curve can be used to calibrate the ratio between the potential measured on the detector and the cantilever deflection in distance units. This slope is usually called deflection sensitivity (Sens) and depends mainly on the cantilever geometry, the laser alignment on the cantilever (and other parameters of the optical path of the beam), and secondarily on temperature gradients. We used the deflection sensitivity measured at the appropriate temperature to convert the raw deflection as follows:

$$\mathrm{Defl/nm} = \frac{\mathrm{Defl/V}}{\mathrm{Sens\ (V/nm)}} \qquad \text{(S.1)}$$

whereDefl is the cantilever deflection (in nm and V).

The conversion of the cantilever deflection to force (F) assumes a simple Hooke-like law (F =-K.Defl, where K is the spring constant of the cantilever).There are several procedures to calibrate the cantilever spring constant (Butt et al., 2005; Attard, 2007). Cleveland et al. (Cleveland et al., 1993) found the following relationship between the spring constant of the cantilever and its resonance frequency and geometric dimensions:

$$K = 2\pi^3 l^3 w \sqrt{\rho^3/E} \nu_0^3 \quad \text{(S.2)}$$

where$l$ and $w$are the length and width of the cantilever, respectively, ρ is its average density, E its Young's modulus,and ν_0 the resonance frequency. Veeco's software includes empirical factors f_{cant} for the conversion $K = f_{cant}\ \nu_0^3$ for the V-shaped cantilevers (SNL, silicon, and DNP, silicon nitride, TableS1). Hence, for V-shaped cantilevers, we measured the resonance frequency under flow of N_2(g) and obtained the spring constant from the software. For rectangular platinum covered cantilevers (SCM-PIC, Table S1), Veeco does not provide f_{cant}. Hence, we calculated its spring constant from ν_0 using a method similar to that proposed by Sader et al. (Sader et al., 1995). Sader et al., (Sader et al., 1995) only uses as parameters the resonance frequency and total mass of the cantilever:

$$K = M_e m (2\pi\nu_0)^2 \quad \text{(S.3)}$$

where M_e is a normalized effective mass (calculated by a finite element resolution of the mechanic equations), and m is the total mass of the cantilever. Using a Poisson ratio = 0.25 and $l / w = 9$ (from the nominal geometry of the tip), we obtained $M_e = 0.2413$ from Fig. 3 of the work by Sader et al. (Sader et al., 1995). We calculated the total mass of the cantilever from its nominal dimensions and densities, and we measured its resonance frequency with the AFM. The frequency had to be corrected to take into account the air resistance, which causes a 4% and 2% damping of ν_0 for V-shaped and rectangular cantilevers, respectively (section III.B in Sader et al., 1995). Finally, in commercial AFM tips, the tip itself is not located at the very end of the cantilever (see Fig. 8 in the main article). Thus, the effective constant is calculated according to the precise position where the force is applied on the cantilever (Sader et al., 1995):

$$K = K_E \left(\frac{L}{L-\Delta L}\right)^2 \quad \text{(S.4)}$$

where$K$ is the spring constant when the load is applied a distance ΔL from the end of the cantilever, K_E is the end tip spring constant and L is the total length of the cantilever. Average values for L and ΔL are provided by the manufacturer.

Force curves are usually presented as a function of z_{tip} (tip to sample distance for negative values or indentation depth for

positive values) in the abscissa axis (lower panel on Fig. S1). The conversion equation is simple:

$$z_{\mathrm{tip}}/\mathrm{nm} = z_{\mathrm{piezo}}/\mathrm{nm} - \mathrm{Defl}/\mathrm{nm} = z_{\mathrm{piezo}}/\mathrm{nm} - \frac{\mathrm{Defl/V}}{\mathrm{Sens/(V/nm)}} \quad \text{(S.5)}$$

We normalized the curves by fixing $z_{\mathrm{tip}} = 0$ at position C in Fig.1S, under the assumption that the contact region begins at that distance. This implies suppositions (Butt, 2005; Attard, 2007) that are~~will be~~ analyzed in the paper text.

Since laser alignment might change during the experiments, which would affect deflection measurements, an additional calibration was performed. After deposition of ice, which does not behave as an "infinitely hard" substrate (Butt et al., 2000; Pittenger et al., 2001), there is no possibility to check if the deflection sensitivity has changed. D'Costa and Hoh (D'Costa and Hoh, 1995) performed several calibrations of the deflection sensitivity on a hard substrate, for slightly different alignments of the laser beam, while keeping the same effective length of the cantilever. They found a linear relationship between the deflection sensitivity, and the shift of the potential (V) for a fixed displacement of the detector in z direction. Figure S2 shows the results of a similar calibration for our AFM. During the experiments, we retracted the tip periodically and checked for modifications in V. In very few cases, we observed a change in V (due to a small change in the laser beam alignment), and in those cases we used the calibration curve to recalculate Sens.

It must be emphasized that one of the main parameters determined in this work, the jump-in distance, is calculated as a difference between z_{tip} distances: $d_{jump-in} = z_{tip}^{C} - z_{tip}^{B}$, where superscript B and C refer to positions of the tip at Fig. S1. Hence, the jump in distance is directly influenced by calibrations of z_{piezo} and *Sens* (from eq. S.5), but does not depend on the calibration of the spring contact or the zero distance definition.

S2. AFM Force Curves

The following figures represent some of the experimental AFM force curves from which results in Table 2 of the main article have been extracted.

Figures S3 and S4 represent continuous force curves measurements performed with silicon nitride tips in the same position over the ice surface, which show high reproducibility. The reproducibility of all the force curves can be captured by considering the averages and standard deviations of their key features (ice indentation slope and jump-in distance) on Table 2.

Figure S5 shows the approach and retract portions of sample force curves measured on ice with platinum covered silicon nitride tips. It can be seen that for these curves the approach portion does not present jump-in, and the retract portion does not presents adhesion (opposite to the large adhesion forces represented in the upper and central~~r~~ panels ~~in~~of Figure 5 ~~of~~in the main article).As we describe in the main article, most of the AFM force curves measured with platinum covered tips or silanized tips on the mEC share these features.

Figure S6 shows one of the few cases when we could measure explicitly the thickness of the ice sample. The thickness canbe

estimated from the difference between the end of the jump-in ($z_{tip} = 0$) and the infinite slope (mica substrate, $z_{tip} \approx 40$ nm). In most of the experiments, ice thicknesses were much larger, therefore the tip did not reach the mica substrate. In those cases, we can only infer a lower bound for the ice thickness (the maximum indentation depth).

References

Attard, P.: Measurement and interpretation of elastic and viscoelastic properties with the atomic force microscope, J. Phys.: Condens. Matter, 19, 473201, 2007.

Butt, H.-J., Döppenschmidt, A., Hüttl, G., Müller, E., and Vinogradova, O. I.: Analysis of plastic deformation in atomic force microscopy: Application to ice, J. Chem. Phys., 113, 1194-1203, 2000.

Butt, H.-J., Cappella, B., and Kappl, M.: Force measurements with the atomic force microscope: Technique, interpretation and applications, Surf. Sci. Rep., 59, 151-152, 2005.

Cleveland, J. P., Manne, S., Bocek, D., and Hansma, P. K.: A nondestructive method for determining the spring constant of cantilevers for scanning force microscopy, Rev. Sci. Instrum., 64, 403-405, 1993.

D'Costa, N. P., and Hoh, J. H.: Calibration of optical lever sensitivity for atomic force microscopy, Rev. Sci. Instrum., 66, 5096-5097, 1995.

Pittenger, B., Fain, S. C., Cochran, M. J., Doney, J. M. K., Robertson, B. E., Szuchmacher, A., and Overney, R. M.: Premelting at ice-solid interfaces studied via velocity-dependent indentation with force microscope tips, Phys. Rev. B., 63, 134102, 2001.

Sader, J. E., Larson, I., Mulvaney, P., and White, L. R.: Method for the calibration of atomic force microscope cantilevers, Rev. Sci. Instrum., 66, 3789-3798, 1995.

Table S1: Nominal parameters of the commercial AFM tips (Bruker/Veeco). *R*: curvature radii of the tip. *K*: force constant, ν_0: resonance frequency and τ: period of the cantilever. For the curvature radii (*R*), maximum values reported by the manufacturer areindicated in brackets.

Material	Model	*R* (nm)	*K* (N/m)	ν_0 (kHz)	τ (μs)
Si	SNL	2 (max 12)	0.06-0.35	18-65	15-56
Si_3N_4	DNP	20 (max 60)	0.06-0.35	18-65	15-56
Si, Pt/Ir	SCM-PIC	20 (max 25)	0.2	13	77

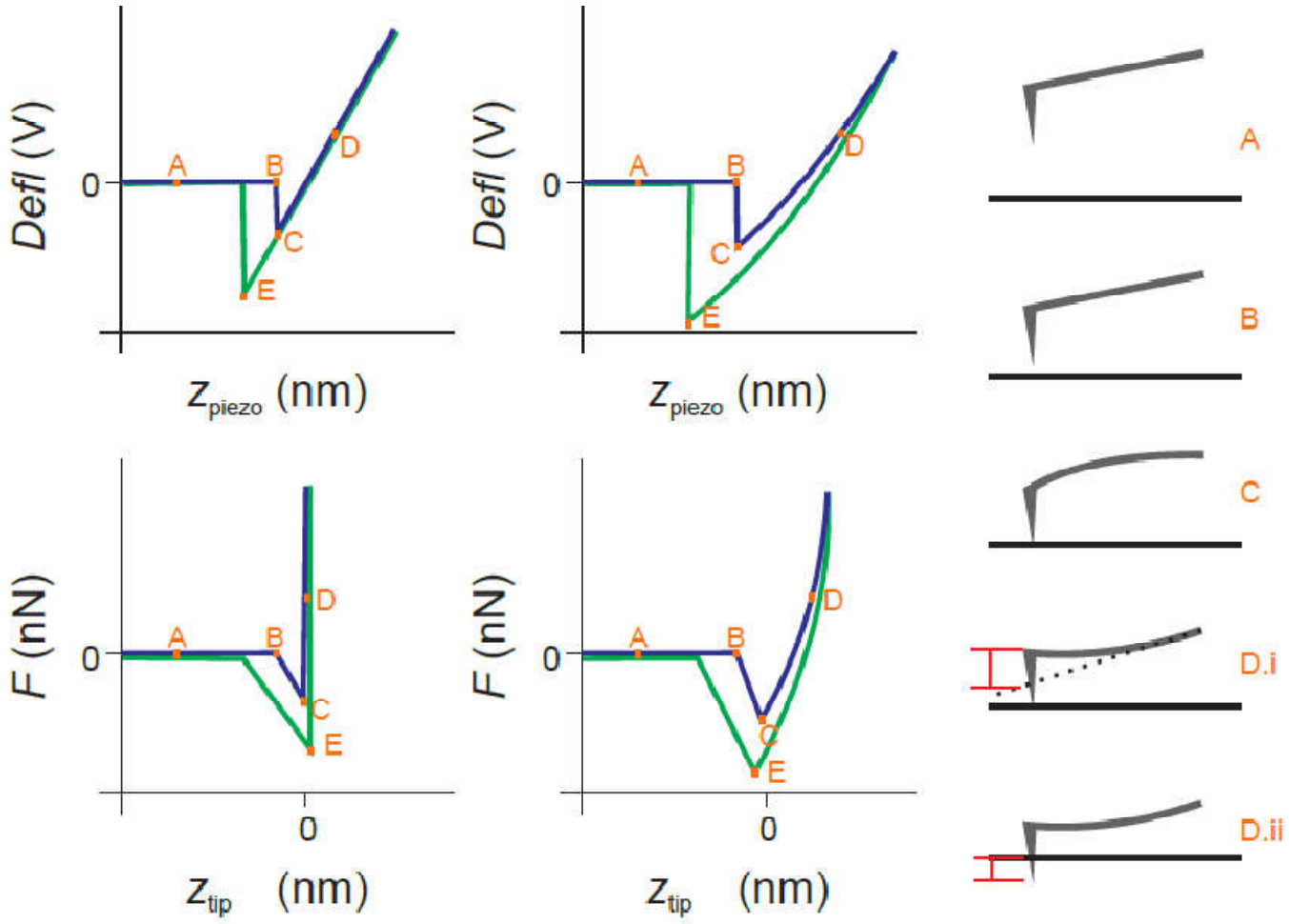

Figure S1: Typical AFM force curves, (approach ~~(),~~ and retract ()). ~~Left~~ panel represents and infinitely hard substrate, while central panel represents a soft sample. The diagrams on the right panel show the tip position and cantilever flexion for different distances indicated with letters on the force curves. The red line in diagram D.i (hard substrate) represents the deflection distance. The red line in diagram D.ii (soft sample) represents the indentation depth.

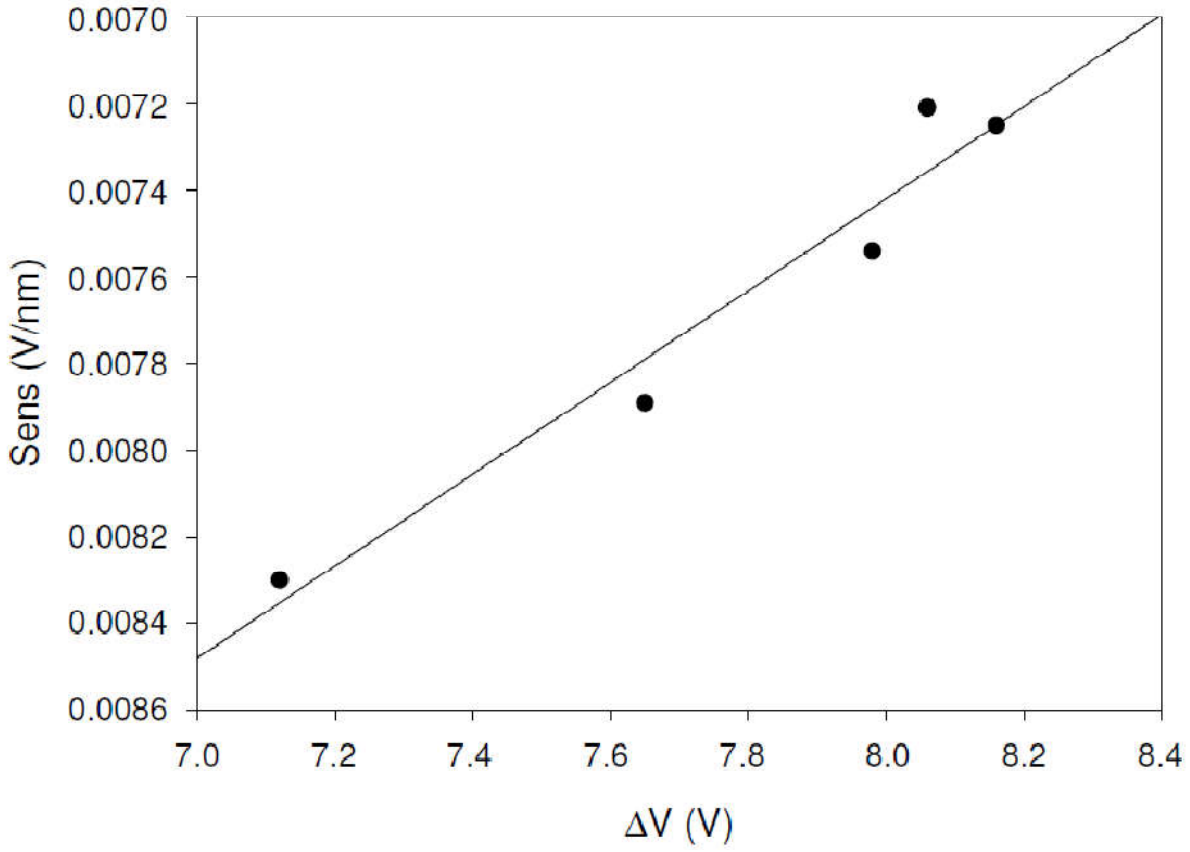

Figure S2:Example of a sensibility (Sens) calibration curve as a function ofvoltage (ΔV), performed with a platinum tip on mica at 4^0C.

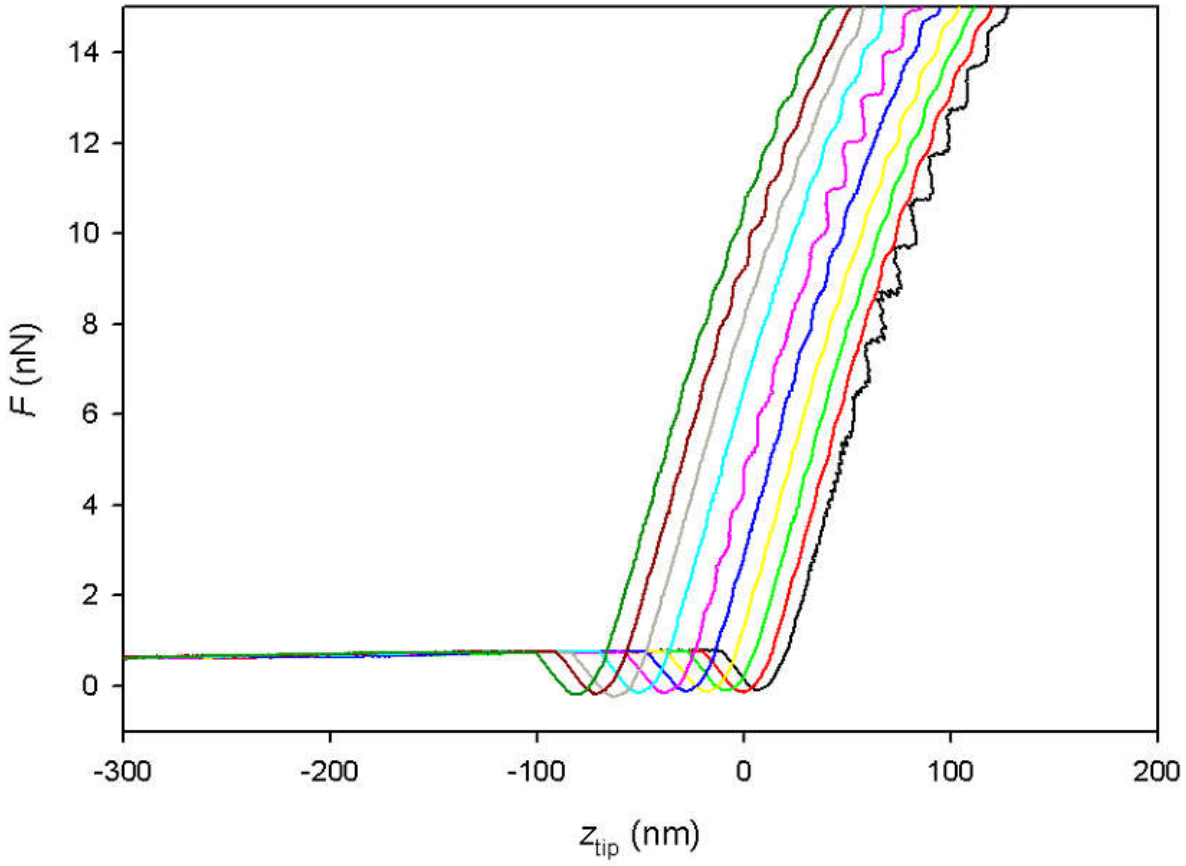

Figure S3: AFM force curves (with jump-in) measured on the same position on the ice surface at -5.0 °C with a silicon nitride tip and the mEC.

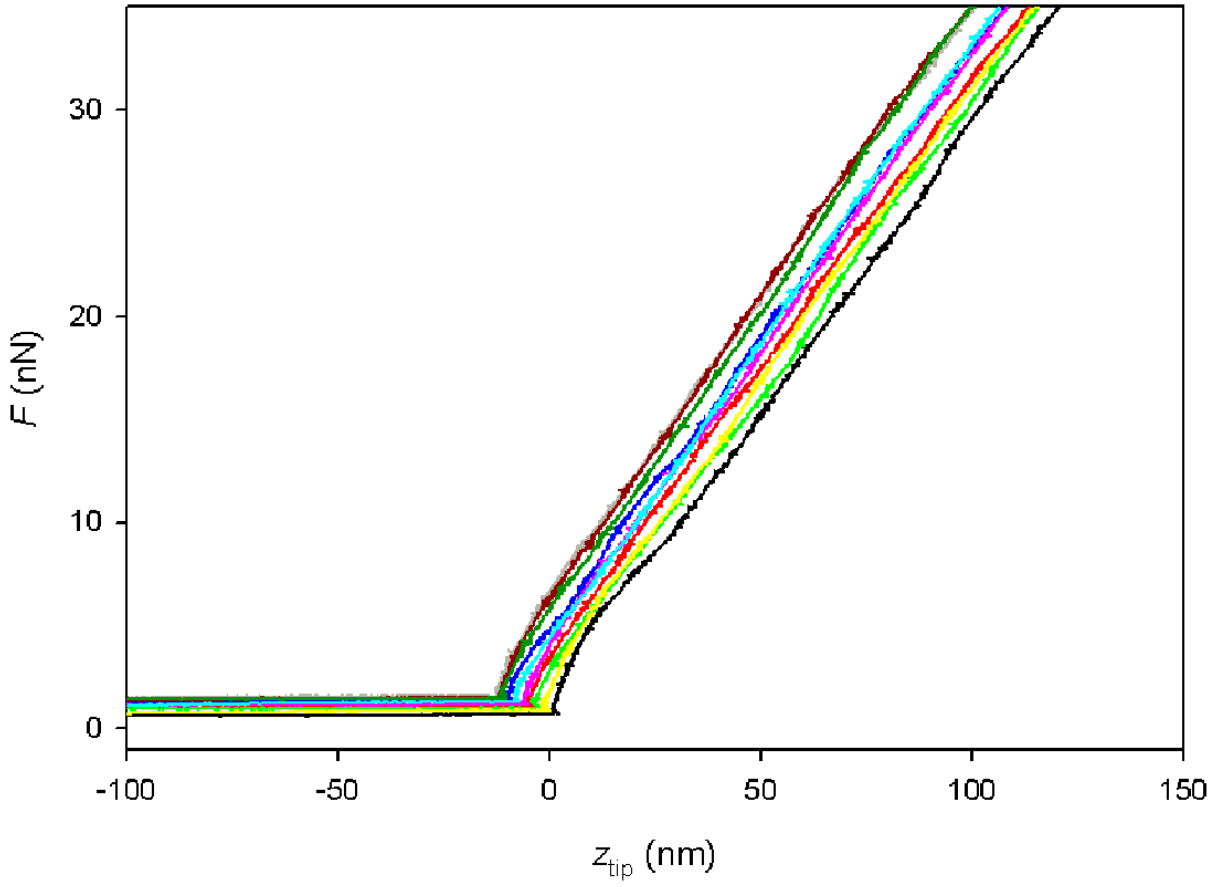

Figure S4: AFM force curves (whithout jump-in) measured on the same position on the ice surface at -2.5 °C with a silicon nitride tip and the mEC.

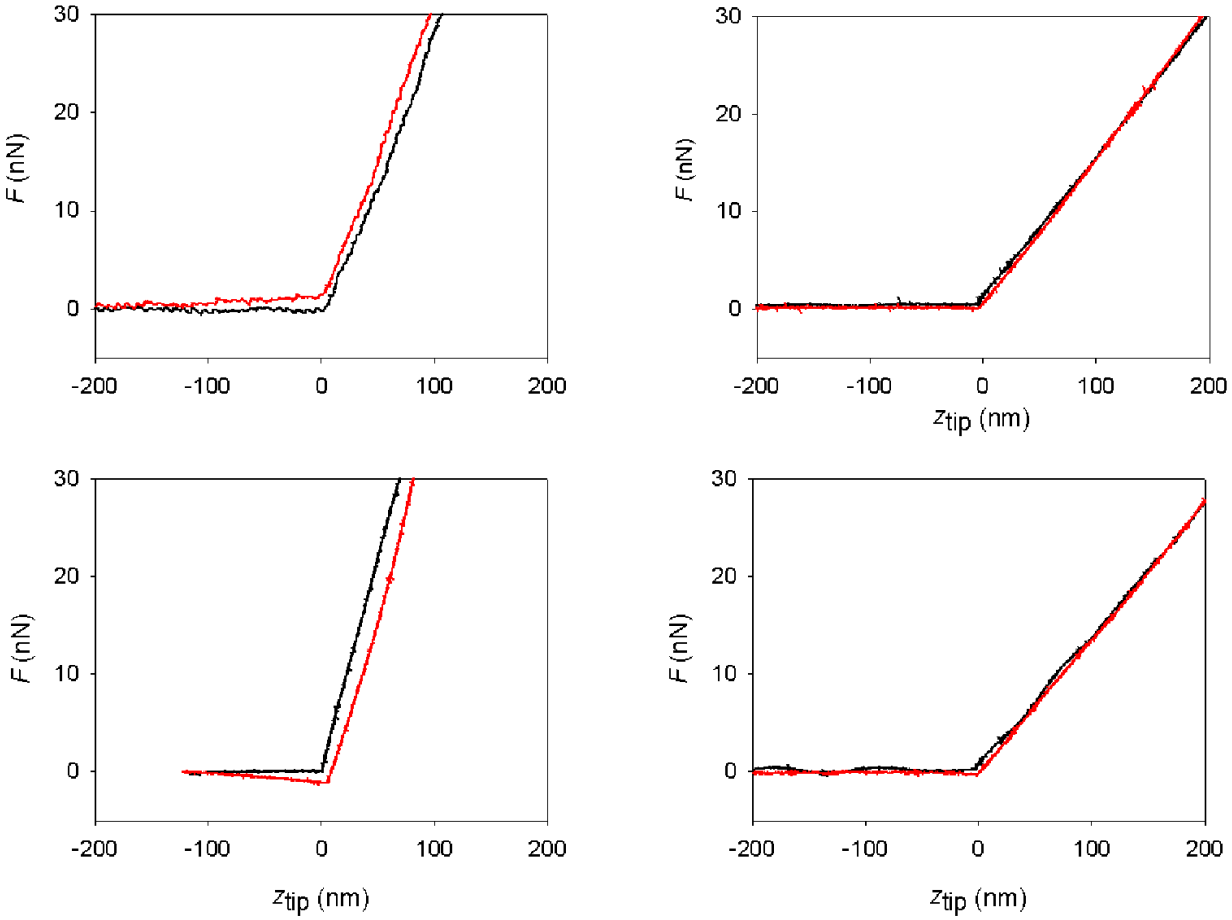

Figure S5: AFM force curves measured with platinum covered silicon nitride tips in the mEC. Top left: -6.5 ºC. Top right: -4.0 ºC. Bottom left: -3.0 ºC. Bottom right: -2.0 ºC. Black lines represent the approach portion of the force curves, whereas the red lines correspond to the retract portion.

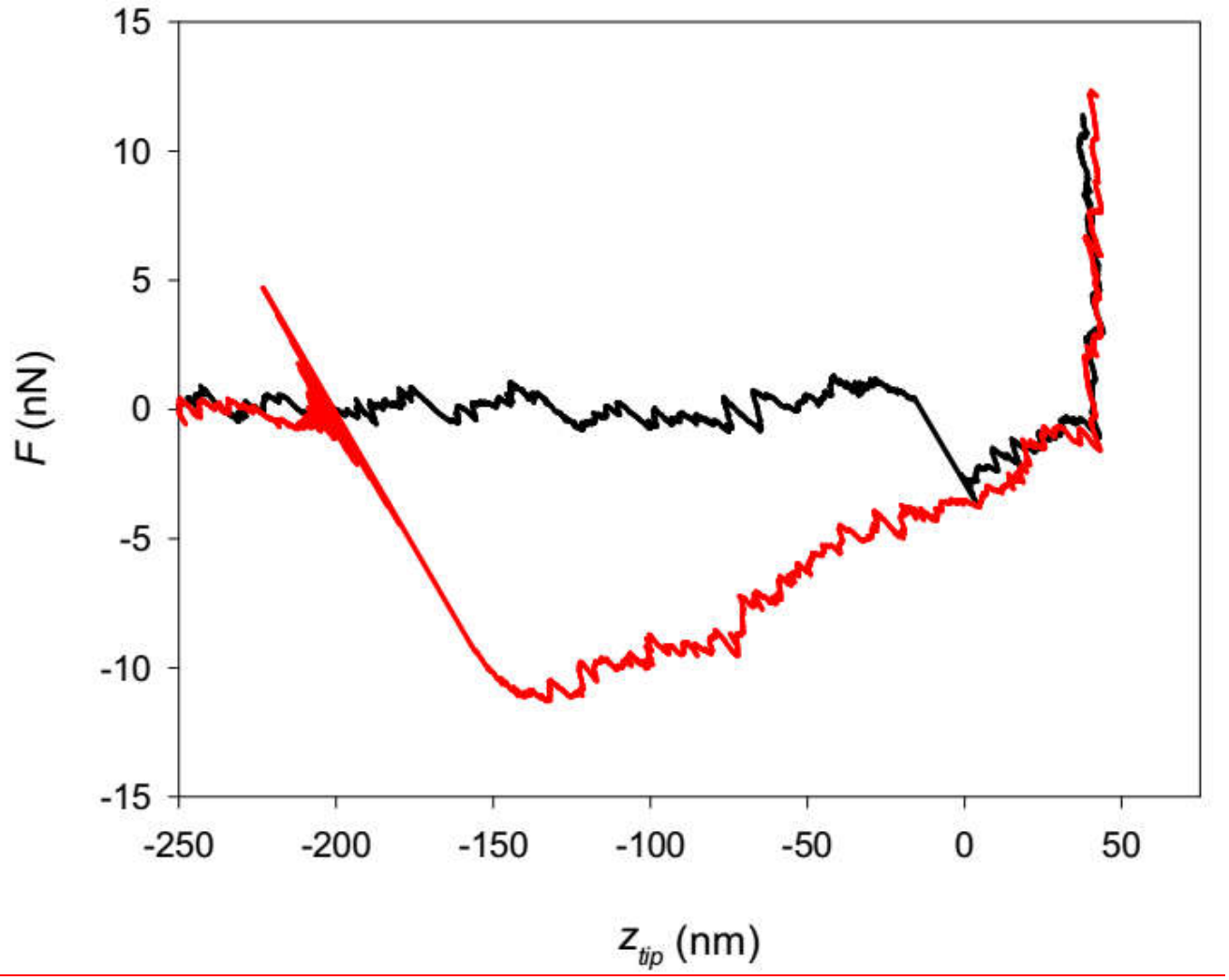

Figure S6:AFM force curve measured at -2.0 ºC with a silicon nitride tip and the mEC. Ice sample thickness can be estimated as the difference between the end of jump-in (z_{tip} = 0) and the infinite slope (mica substrate, z_{tip}≈ 40nm). The black curve corresponds to the approach portion of the force curve and the red one to the retract portion.